AC

EUROPEAN ORGANIZATION FOR NUCLEAR RESEARCH

CERN AT/94-10 (DI)

Diffractive Beauty Production at the LHC Collider

K. Eggert and A. Morsch

Abstract

Using the framework of Pomeron exchange to describe diffractive pp collisions at the LHC we discuss the beauty production in those events. The cross-sections for beauty production at different diffractive masses and the topology for the beauty particles and the underlying event are given. When triggering on large diffractive masses the beauty system is boosted into the Pomeron hemisphere opposite to the underlying event which follows closer the excited proton direction. This may offer some advantages for the beauty acceptance and the reconstruction in forward spectrometers.

Geneva, Switzerland
9 September 1994

1. Introduction

Inelastic diffractive processes in which one of the two protons stay intact but looses momentum have been studied at the ISR [1] and the proton-antiproton collider [2]. It is currently believed that single diffraction is mediated by a Pomeron which, being a part of one proton, interacts with the other proton and thus produces an excited system with mass M recoiling against the intact proton (Fig. 1a,b). The Pomeron has taken the fraction ξ of the proton momentum leaving a proton with a beam momentum fraction $x=1-\xi$. The mass M of the system X in which the other proton is excited is related to this relative momentum loss $\xi = \Delta p / p_0$ by

$$1 - x = \xi = \frac{M^2}{s} \qquad (1)$$

where $\sqrt{s}=2p_0$ is the centre of mass energy of the collision. At the LHC ($\sqrt{s}$=14 TeV) the physical meaningful range of ξ is covered by:

$$\frac{(m_p + m_\pi)^2}{s} < \xi < \frac{m_\pi}{m_p} \Leftrightarrow \qquad 6\ 10^{-9} < \xi < 0.15 \qquad (2)$$

The largest momentum loss leading to an excited mass of around 4 TeV or a Pomeron momentum of above 1 TeV is limited by the coherence condition, whereas the lowest mass corresponds to the production of one additional pion. The momentum loss of the proton in diffractive events at the LHC is therefore in the range of 10^{-8} to 10^{-1}.

As described in Ref. [3], the proton momentum loss ξ can be measured in the range of 10^{-3} to 10^{-1} by means of Roman pots placed upstream in the straight section. In such a way a Pomeron beam can be defined with momenta between 10 and 1000 GeV. Often the Pomeron is seen as a multi-gluon state. Measurements indicate that its structure function seems to be rather hard [4]. Thus the hard gluon beam from the Pomeron interacts with the proton constituents.

Heavy flavours, like beauty and top, are mainly produced by gluon interactions. It is therefore an interesting question to ask whether the possibly enhanced gluon flux in diffractive events would lead to a substantial heavy flavour production. The topology of diffractive events with most of the particles going along the diffractive system is quite different from the one of normal pp events. It is therefore not excluded that the kinematics and the signal-to-background ratio for beauty particles may be more favourable in these events.

In Fig. 1c, the pseudo rapidity distributions of particles from two different excited masses are sketched. The lower the mass the more forward the particles are emitted into the hemisphere opposite to the Pomeron. Low mass diffraction (M < 0.5 TeV) with proton momentum losses, which cannot be directly detected, can thus be identified by the presence of a pseudorapidity gap, a method frequently used in the past.

2. Simulation of Diffractive Hard Scattering

To simulate heavy flavour production in single diffractive pp interactions we used PYTHIA 5.7 [5] in combination with POMPYT, a special diffractive event generator built by G. Ingelman *et al.* [6].

The differential cross section for pp diffractive hard scattering is:

$$\frac{d\sigma(pp \to Q\bar{Q}X)}{d\xi dt dx_i dx_j d\hat{t}} = f_{\mathbb{P}/p}(\xi,t)\frac{d\sigma(p\mathbb{P} \to Q\bar{Q}X)}{dx_i dx_j d\hat{t}} \tag{3}$$

The first term on the right side is the pomeron flux factor and the second one the differential cross section of the hard scattering between the Pomeron and the proton. Here, x_i and x_j denote the momentum fractions of the interacting partons and ξ the momentum fraction of the Pomeron; t is the transverse momentum squared transferred by the Pomeron and $\hat{t}$ symbolises an independent set of Mandelstam variables.

As described in Ref. [7], the Pomeron flux factor was calculated from the t-dependence of the proton form factor $F_1(t)$ and an $1/\xi$ dependence:

$$f_{\mathbb{P}/p}(\xi,t) = \frac{1}{\sigma(p\mathbb{P} \to X)}\frac{d\sigma}{d\xi dt} = \frac{C}{\sigma(p\mathbb{P} \to X)}\cdot\frac{1}{\xi}[F_1(t)]^2 \tag{4}$$

with $$F_1(t) = \frac{4m_p^2 - at}{4m_p^2 - t}\left(\frac{1}{1-t/b}\right)^2$$

and a=2.8, b=0.7 GeV^2. $\sigma(p\mathbb{P} \to X)$ =2.3 mb is the total Pomeron proton cross section. The normalisation constant C was set to 2.3 mb GeV^{-2} corresponding to a total single diffractive cross section of 12 mb/side.

Integrating over t and ξ one obtains for the total diffractive cross section in the pomeron momentum range $\xi_{min}<\xi<\xi_{max}$:

$$\sigma_{SD}(\xi_{min} < \xi < \xi_{max}) = 0.7\text{mb } \ln\left(\frac{\xi_{max}}{\xi_{min}}\right) \tag{5}$$

The hard scattering cross-section is a product of the proton and Pomeron structure functions and the parton-parton cross section.

$$\frac{d\sigma(p\mathbb{P} \to Q\bar{Q}X)}{dx_i dx_j d\hat{t}} = f_{g_i/p}(x_i,Q^2) f_{g_j/\mathbb{P}}(x_j,Q^2)\frac{d\sigma_{ij}}{d\hat{t}} \tag{6}$$

We assume that the dominant structure of the Pomeron consists of gluons, although this is still an open question. The 'hard' structure function advocated by Ingelman and Schlein [4] was used for the calculations and a soft structure function for comparison:

$$
\begin{aligned}
zf_{g/\mathbb{P}}(z) &= 6z(1-z) && \text{(hard gluons)} \\
zf_{g/\mathbb{P}}(z) &= 6(1-z)^5 && \text{(soft gluons)}
\end{aligned}
\qquad (5)
$$

3. Diffractive Heavy Flavour Cross-sections

In Fig. 2a, the differential cross-sections $d\sigma/dM$ for the inclusive production of the diffractive mass M and for beauty production in this mass bin is plotted versus $\log\xi$ having in mind that the diffractive cross-section is constant (~1.5 mb/decade) in equal bins of $\log\xi$. On the contrary, the beauty cross-section increases by two orders of magnitude over the mass range (Fig. 2b), reaching at the highest masses a beauty fraction of 0.6% which is similar to pp collisions at $\sqrt{s}$=14 TeV and more than a factor 100 times larger than in an LHC fixed target scenario. With the soft gluon structure function of the Pomeron this beauty fraction would even exceed 2% at the highest masses. The charm-to-beauty ratio approaches at large masses 10-20, also similar to normal pp collisions ($\sqrt{s}$=14 TeV), whereas it is above 100 at low diffractive masses (Fig. 3).

In our assumed scenario, in which the Pomeron consist of hard gluons, the beauty and charm content in diffractive events with a sub energy of ~ 1 TeV is comparable to the one in normal events, but at the larger energy of 14 TeV. It has now to be seen whether diffractive events with an excited mass around 1 TeV, emitted opposite to the Pomeron, have a topology which allows an easier distinction of the beauty particles compared to normal pp events. We therefore study in the next chapter the topology of these events.

4. Topology of Diffractive Beauty Events

The following figures illustrate the beauty kinematics with respect to the underlying event. The average pseudorapidity η and the η-range for beauty and the particles from the underlying event are shown in Fig. 4 for (a) the hard and (b) the soft gluon structure functions. Positive pseudorapidities denote the hemisphere of the excited proton, negative ones of the Pomeron. Whereas for the soft structure function the beauty particles follow the underlying diffractive event the distributions are quite different for the hard structure function, in particular at large masses. At low masses the beauty particles and the underlying event particles go together into the excited proton hemisphere. With increasing diffractive masses the particle distribution gets wider and the beauty particles move into the opposite hemisphere, following the Pomeron direction (Fig. 5). When the Pomeron takes a substantial fraction of the proton momentum (1-10%) the gluons in the Pomeron have, on average, larger momenta than the ones in the proton and hence the beauty particles are boosted along the Pomeron direction. From the experimental point of view this has two advantages: by choosing a large diffractive mass the beauty particles with a pseudorapidity distribution extending over only a few units can be boosted into the acceptance of the apparatus. Secondly, most of the underlying event particles are in the proton hemisphere thus reducing the combinatorial background for beauty reconstruction.

Fig. 6 shows the acceptance of the $b\bar{b}$ pairs as a function of $\log\xi$ for different assumed spectrometer apertures. As an example, the forward (600 mrad) COBEX detector (Ref. [8]), placed in the Pomeron hemisphere, accepts more than 60% of the $b\bar{b}$ pairs in high mass diffraction with most of the beauty particles being even within 200 mrad. In the proton hemisphere, COBEX would almost fully cover the diffractive beauty production for masses below 0.3 TeV.

The average beauty momentum , shown in Fig. 7, is around 50 GeV for large masses (M >3 TeV) and increases above 100 GeV at masses below 0.1 TeV. The momentum distributions of the underlying event particles and the beauty particles are shown in Fig. 8 for three mass bins. The beauty momenta are lowest for diffractive masses around 1 TeV.

5. Summary

The beauty production in high mass diffractive events is as large as in normal pp collisions at $\sqrt{s}$=14 TeV, despite the fact that the sub energy in diffractive events is lower. It may be that, with most of the particles going opposite to the beauty particles (in the case of a hard structure function and large masses), the kinematics and the signal-to-background ratio is more favourable in these events. The relative momentum loss of the protons can be measured in the range of 10^{-3} to 10^{-1} with the help of Roman pot spectrometers. By choosing the proton momentum loss and hence the diffractive mass already on the 1. level trigger, the beauty particles can be boosted into the acceptance of a forward spectrometer, like e.g. the COBEX spectrometer. It has to be further studied whether such a beauty sample would be cleaner compared to normal events.

In any case, beauty production in diffractive events would serve as an ideal tool to study the nature of diffraction and, if the Pomeron would be a quasireal particle, to perform detailed studies of the Pomeron structure. By equipping both forward arms with Roman pot spectrometers double pomeron exchange reactions can be studied. The pp collider could thus be transformed into a Pomeron-Pomeron collider with a sub energy of about 1 TeV thus providing very high momentum gluon-gluon interactions over a probably much reduced background from the underlying event.

References

[1] M.G. Albrow *et al.*, Nucl. Phys. **B108** (1976) 1.

[2] M. Bozzo *et al.*, Phys. Lett. **B136** (1984) 217.

[3] K. Eggert and A. Morsch, '*Leading Proton Detection in Diffractive Events for an LHC Low-β Insertion*', CERN AT/94-09 (DI).

[4] G. Ingelman and P. Schlein, Phys. Lett. **152B** (1985) 256.

[5] H.-U. Bengtsson, T. Sjöstrand, Comp. Phys. Comm. **46** (1987) 43.
T. Sjöstrand, Comp. Phys. Comm. **39** (1986) 347, *ibid*. **43** (1987) 367.

[6] P. Bruni and G. Ingelman, 'POMPYT version 1.0- A Monte Carlo to simulate Diffractive Hard Scattering Processes', DESY 93.

[7] A. Donnachie and P.V. Landshoff, Nucl. Phys. **B303** (1988) 634.

[8] COBEX Letter of Intent, CERN/LHCC/93-50.

Figure Captions

Fig. 1
(a) The initial state momentum vectors in the overall centre-of-mass of the single diffractive reaction p+p→ p+X.
(b) Single diffractive reaction represented by a t-channel *Pomeron* exchange diagram.
(c) Sketch of the single-diffractive event topology for two different diffractive masses *M*.

Fig. 2
(a) Total diffractive cross-section *vs.* log(ξ) (solid curve) and diffractive $b\bar{b}$ cross-section (dotted curve) assuming a hard gluon structure function of the Pomeron.
(b) Ratio of $b\bar{b}$ to total diffractive cross-section.

Fig. 3
Ratio of $c\bar{c}$ to $b\bar{b}$ cross-section.

Fig. 4
The average pseudo rapidity for beauty particles (points) and underlying event particles (line) for **(a)** hard gluon structure and **(b)** soft gluon structure function. The vertical lines show the range of coverage of the underlying event and the width of the beauty particle distribution.

Fig. 5
Particle density distribution *vs.* pseudo rapidity for underlying event and beauty particles assuming a hard gluon structure function for **(a)** diffractive mass *M*=0.2 TeV, **(b)** *M*=1.4 TeV and **(c)** *M*=3.6 TeV. The recoil protons show up at the right-hand side of the plots.

Fig. 6
Beauty-antibeauty pair acceptance for forward spectrometers with 600 mrad (solid line), 200 mrad (dashed line) and 100 mrad (dotted line) aperture.

Fig. 7
Average momentum of the beauty particles *vs.* log(ξ) for **(a)** hard gluon structure and **(b)** soft gluon structure function.

Fig. 8
Particle rate per event *vs.* momentum for underlying event and beauty particles assuming a hard gluon structure function for **(a)** diffractive mass *M*=0.2 TeV, **(b)** *M*=1.4 TeV and **(c)** *M*=3.6 TeV. The recoil protons show up at the right-hand side of the plots.

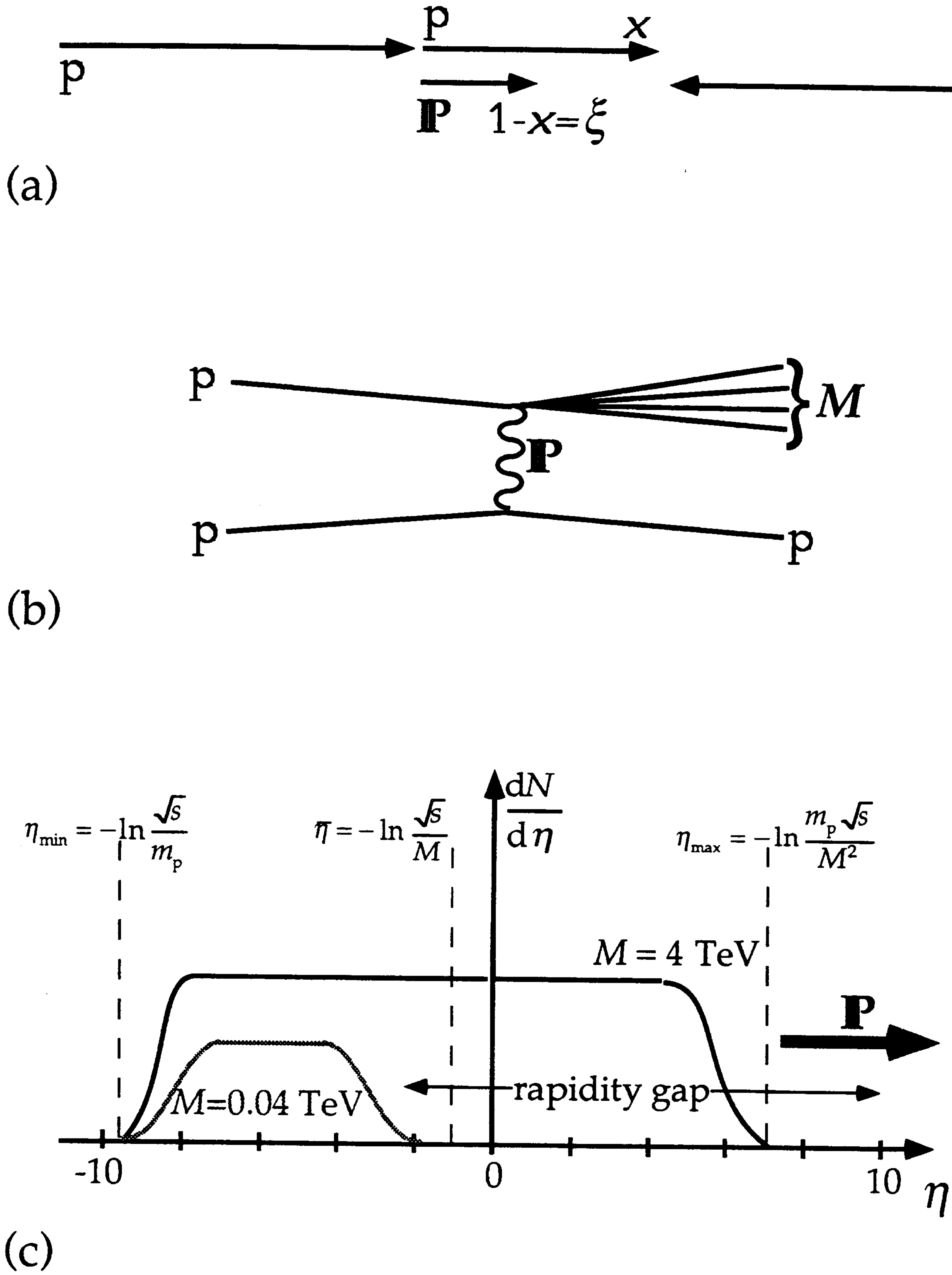

p
p
x
P
1-x=ξ
p
(a)
p
M
P
p
p
(b)
dN/dη
η_min = −ln √s/m_p
η = − ln √s/M
η_max = −ln m_p√s/M²
M = 4 TeV
P
M=0.04 TeV
rapidity gap
-10
0
10
η
(c)

Fig. 1

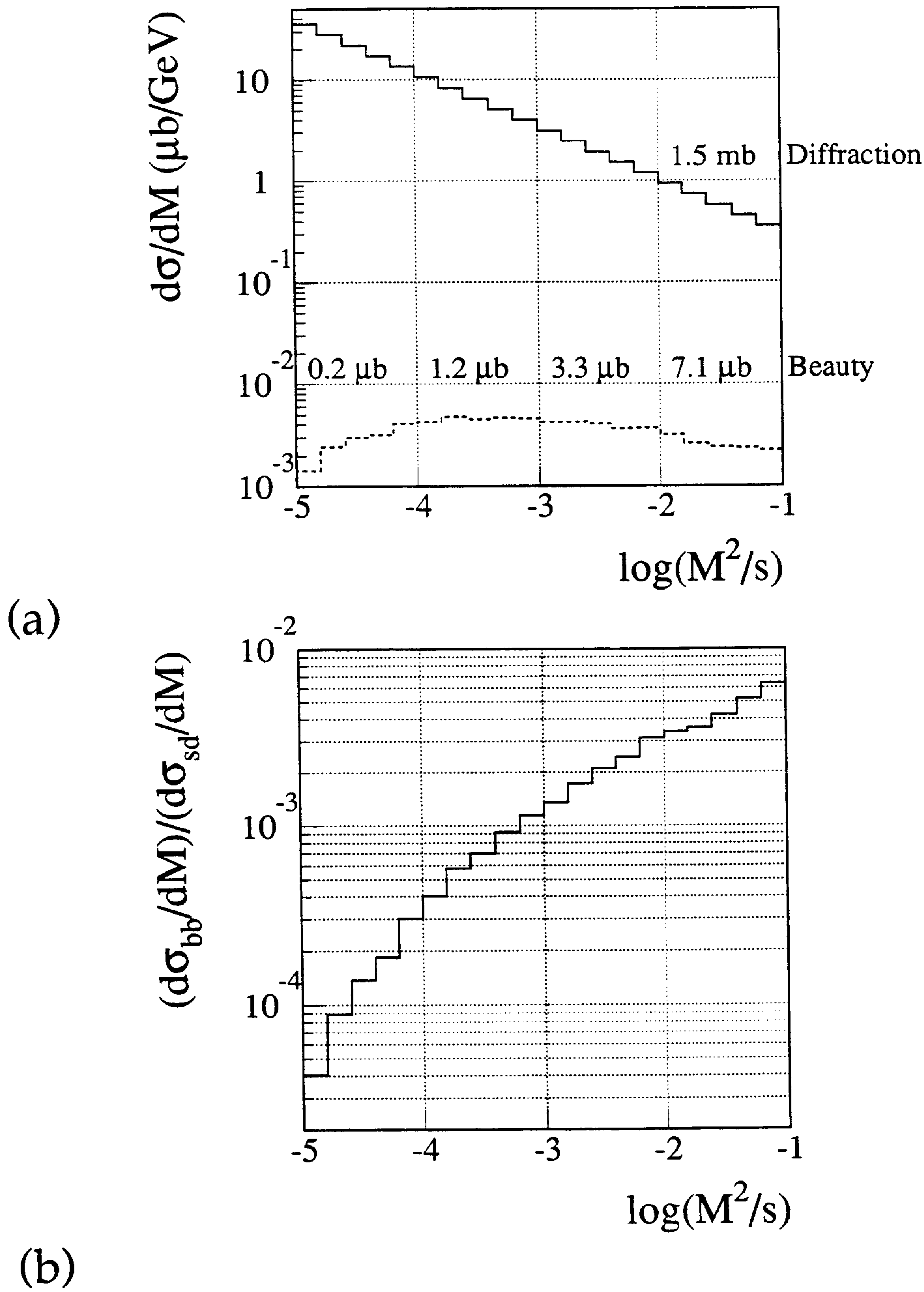

dσ/dM (μb/GeV)
10
1
10^-1
10^-2
10^-3
1.5 mb
Diffraction
0.2 μb
1.2 μb
3.3 μb
7.1 μb
Beauty
-5
-4
-3
-2
-1
log(M^2/s)
(a)
(dσ_bb/dM)/(dσ_sd/dM)
10^-2
10^-3
10^-4
-5
-4
-3
-2
-1
log(M^2/s)
(b)

Fig. 2

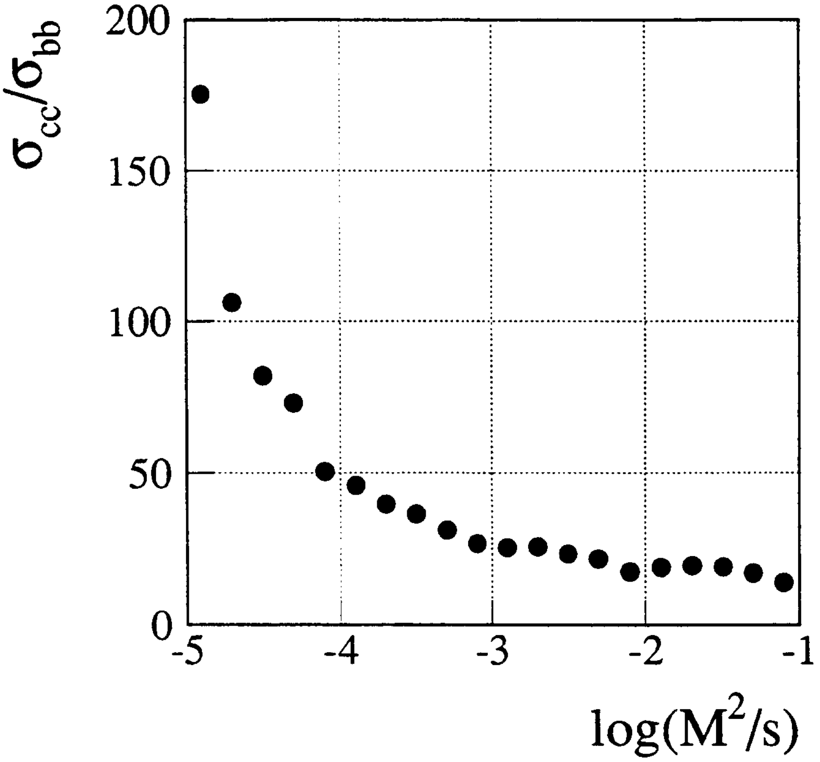

Fig. 3

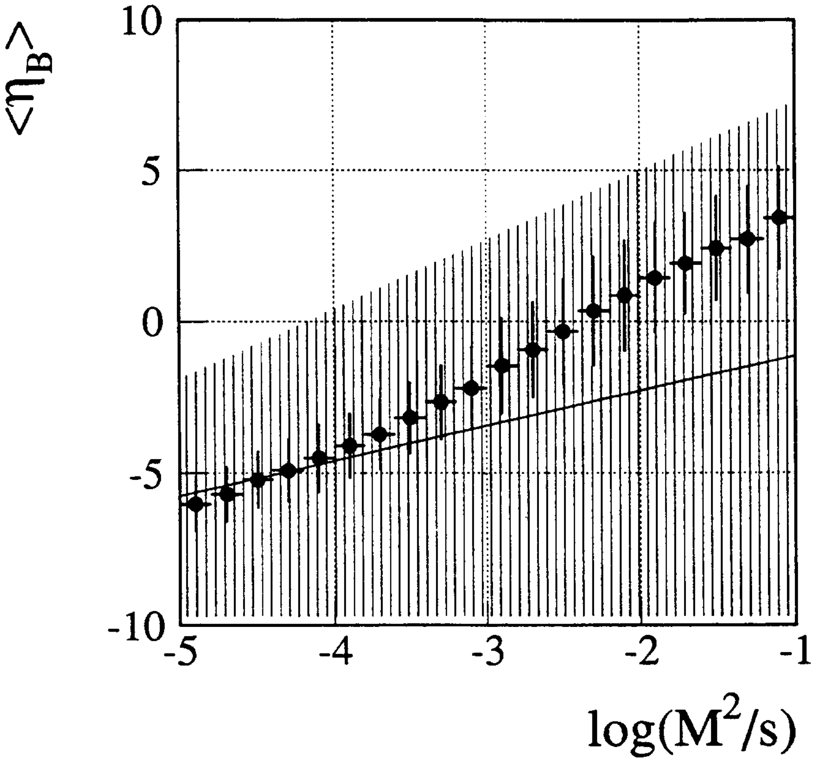

(a)

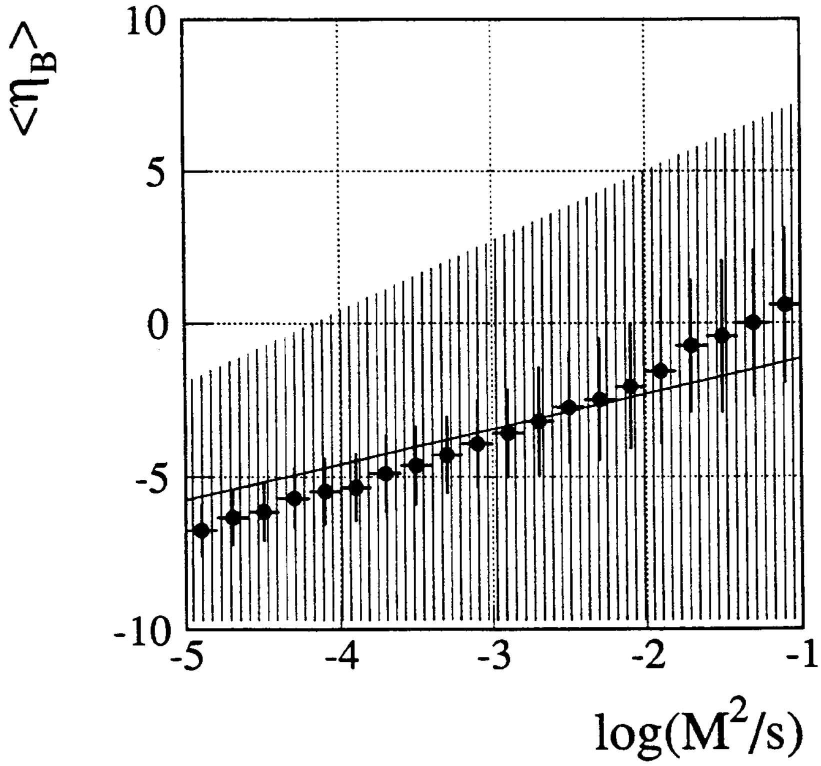

(b)

Fig. 4

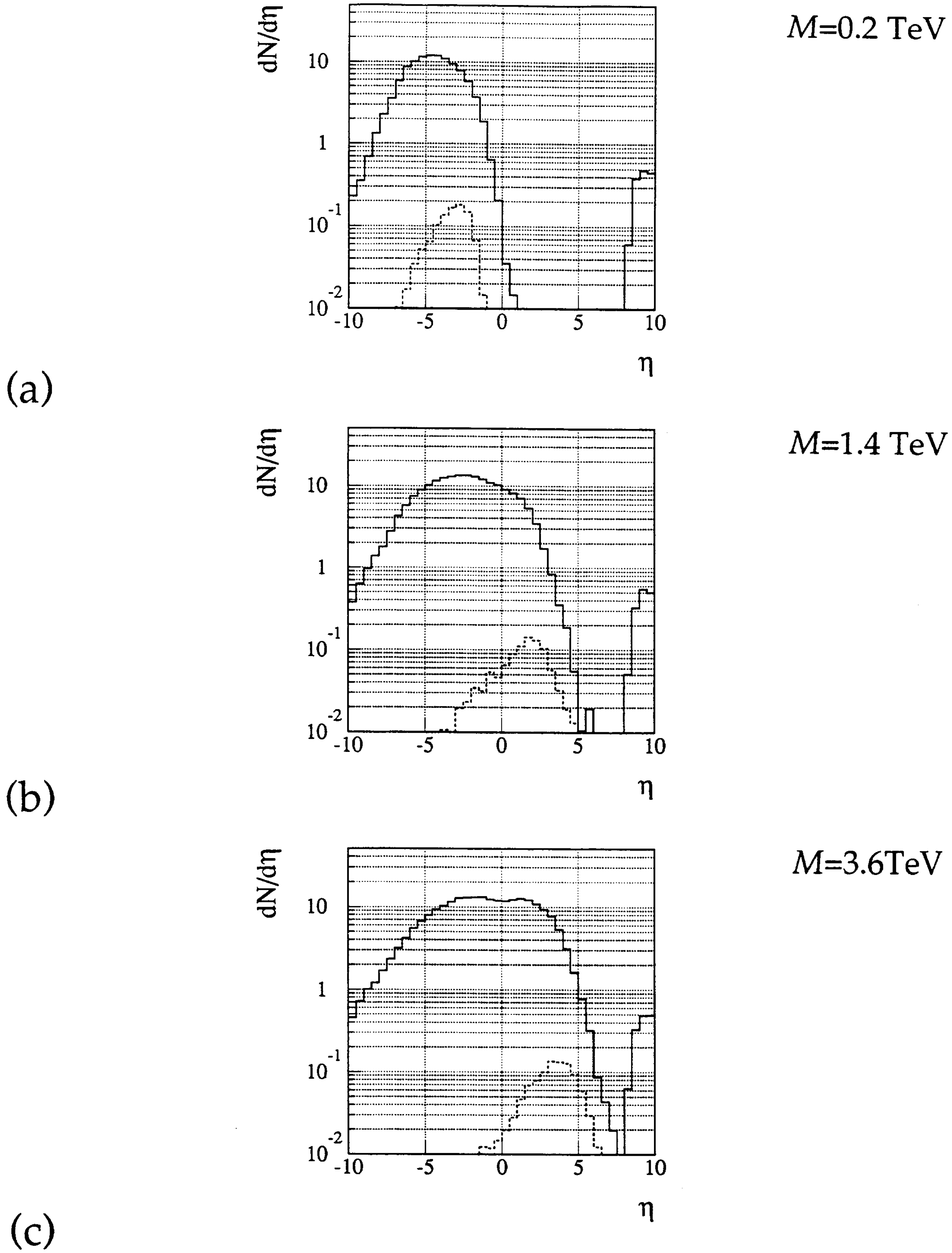
dN/dη
M=0.2 TeV
10
1
10^-1
10^-2
-10
-5
0
5
10
η
(a)
dN/dη
M=1.4 TeV
10
1
10^-1
10^-2
-10
-5
0
5
10
η
(b)
dN/dη
M=3.6TeV
10
1
10^-1
10^-2
-10
-5
0
5
10
η
(c)

Fig. 5

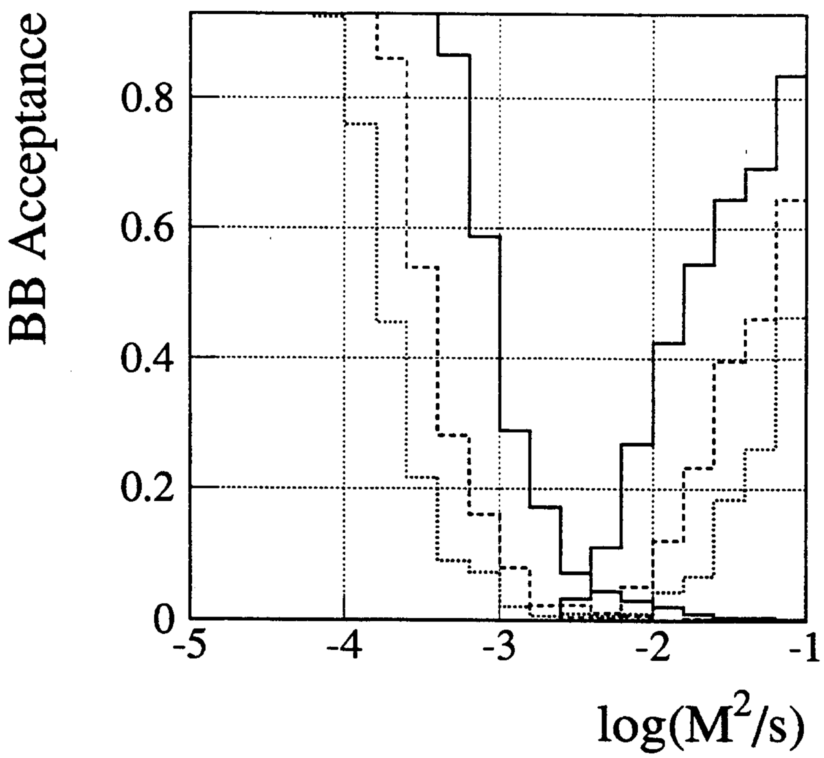

Fig. 6

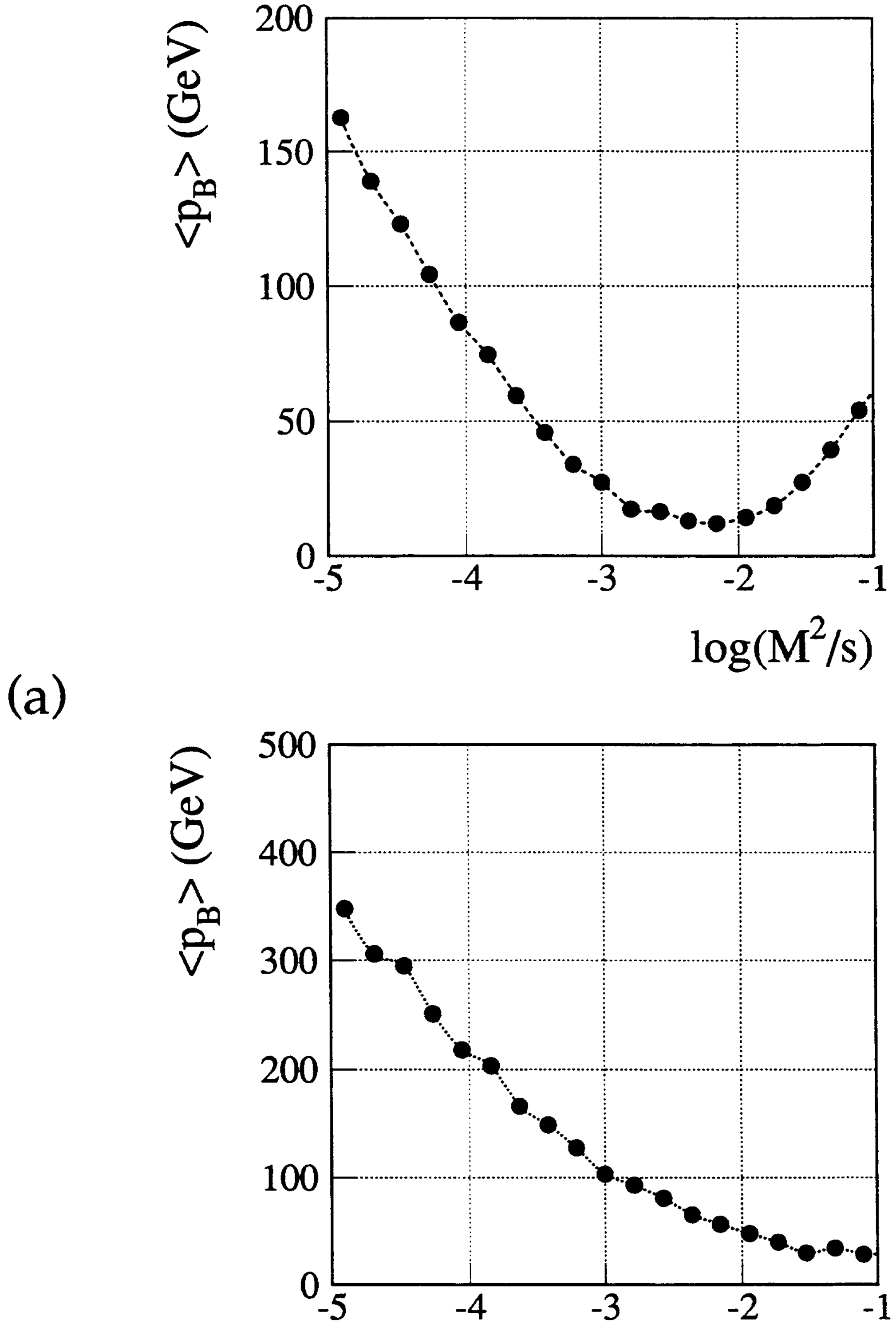

200
150
100
50
0
$<p_B>$ (GeV)
-5
-4
-3
-2
-1
$\log(M^2/s)$
(a)
500
400
300
200
100
0
$<p_B>$ (GeV)
-5
-4
-3
-2
-1
$\log(M^2/s)$
(b)

Fig. 7

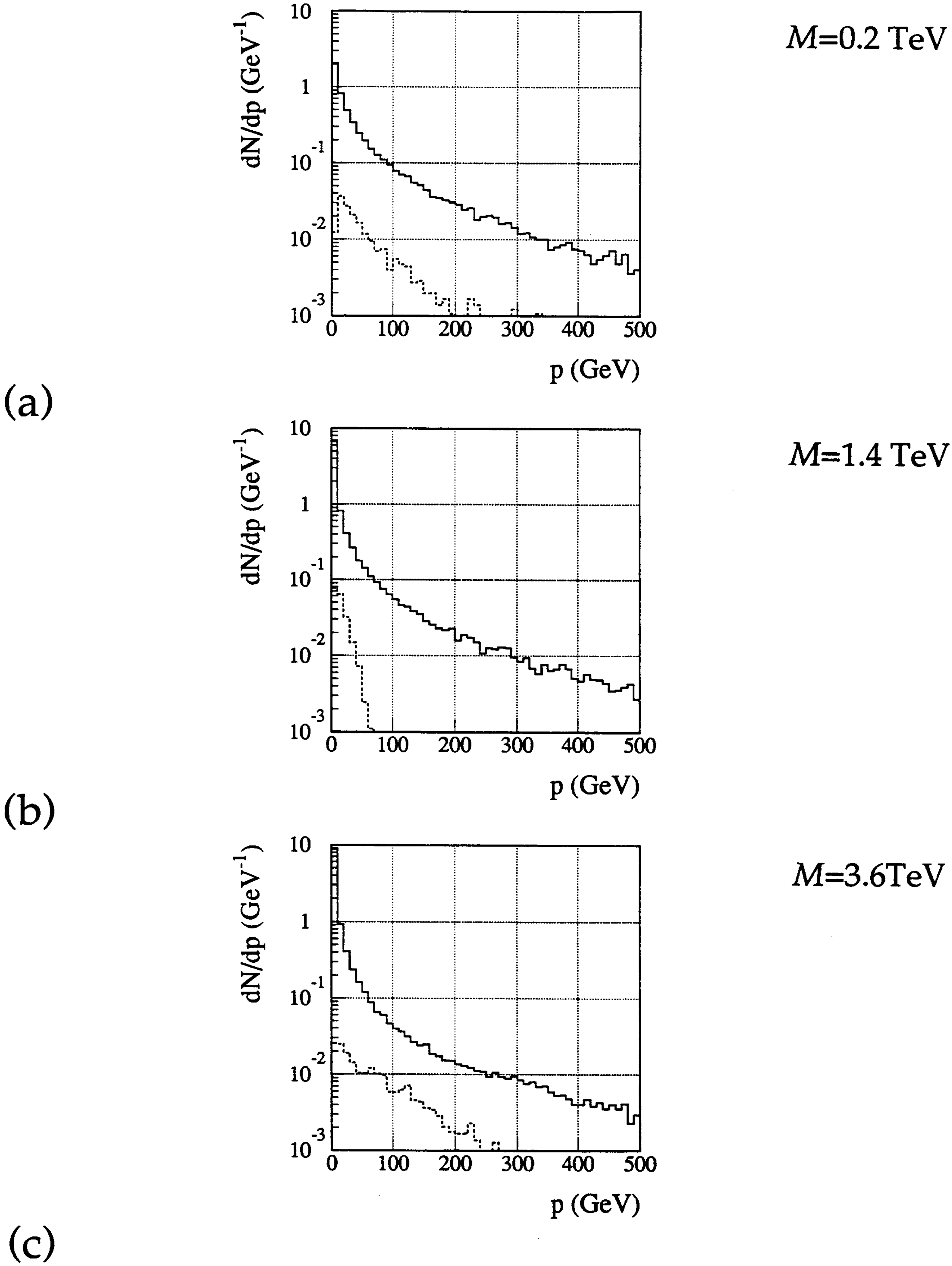

Fig. 8